

## Preliminary Geochemical Characterization of a Low-enthalpy Hydrothermal Reservoir not Associated with Recent Volcanism in Southeastern Sierra Madre Occidental, Mexico

<sup>1</sup>Andrea Billarent, <sup>1</sup>Gilles Levresse, <sup>2</sup>Claudio Inguaggiato, <sup>1</sup>Luca Ferrari, <sup>1</sup>Eliseo Hernández, <sup>1</sup>Juan Carlos Castillo-Reynoso, <sup>1</sup>Emma Vanessa Martínez-Resendiz, <sup>3</sup>Salvatore Inguaggiato, <sup>1</sup>Teresa Orozco, <sup>4</sup>Antonio Hernández-Espriú, <sup>4</sup>Alberto Arias

<sup>1</sup> Centro de Geociencias. UNAM Campus Juriquilla Blvd. Juriquilla 3001. Querétaro 76230, México. <sup>2</sup> Departamento de Geología, Centro de Investigación Científica y de Educación Superior de Ensenada (CICESE), Carretera Ensenada-Tijuana 3918, Ensenada, Baja California, México. <sup>3</sup> Istituto Nazionale di Geofisica e Vulcanologia, Sezione di Palermo, via Ugo La Malfa, 143, 90145 Palermo, Italy. <sup>4</sup> Hydrogeology Group, Earth Sciences Division, Faculty of Engineering Universidad Nacional Autónoma de México (UNAM), México.

andreabillarent@geociencias.unam.mx; glevresse@geociencias.unam.mx

**Keywords:** low-enthalpy, aquifer, graben, isotopy, helium

### ABSTRACT

This work presents the hydrogeochemical results of water and dissolved gas samples collected from thermal and cold groundwater in two grabens in the southern Sierra Madre Occidental of central Mexico. Thermal springs in the Juchipila and the Santiago Papasquiaro grabens reach temperatures of 60 and 74°C, respectively. These geothermal manifestations are not related to recent or active volcanism, as all the known geothermal fields in Mexico.

The thermal waters collected in the Juchipila graben are Na-HCO<sub>3</sub> and Na-SO<sub>4</sub> type and the waters collected in the Santiago Papasquiaro graben are Na-HCO<sub>3</sub> water-type. In both grabens, the thermal samples have anomalous concentration of F, B, Li, and As, associated with rock alteration and dissolution processes. The cold waters have a Ca-HCO<sub>3</sub> composition and chemical characteristics of recent recharge and superficial flow.

The  $\delta^2\text{H}$  and  $\delta^{18}\text{O}$  data indicate a meteoric source for the thermal and cold waters in both grabens, with no volcanic input to the systems. The thermal samples in the Santiago Papasquiaro graben fall on the GMWL, whilst the samples in the Juchipila graben distribute along an evaporation line. In the Juchipila graben, the He composition is mainly of atmospheric origin with a mantle helium contribution up to 14%. On the other hand, the He isotope composition in the Santiago Papasquiaro graben is crustal dominated, with a contribution up to 96%, and characterized by a mantle proportion up to 9%. This implies that in both grabens the fault systems have deep roots or fluids interact with crustal faults, although to a lesser extent in the Santiago Papasquiaro graben.

Based on our results we propose a hydrothermal system model for the Juchipila graben, in which rainwater infiltrates deeply through the graben border fault system, dissolve mantle and crustal helium, and eventually surge at surface along faults cutting the whole succession within the graben. The model for the Santiago Papasquiaro graben is similar, although the high contribution of crustal He implies an alternative/additional heat source, probably related to radioactive decay of U-rich geologic units.

### 1. INTRODUCTION

In Mexico, geothermal studies traditionally focused on conventional fields whose heat source is related to recent and active silicic volcanic systems (e.g. Los Azufres, Los Hornos, and Tres Vírgenes), or to pull-apart basins located along the plate boundary with high heat flux and a thick sedimentary fill (e.g. Cerro Prieto) (Flores-Armenta, 2012; Gutierrez-Negrín et al., 2015; Gutierrez-Negrín and Lipman, 2016). The national need to rapidly increase the production of clean energy, urges the academic community to rethink energy generation models to include the exploration of new, unconventional sources of geothermal energy and to propose an updated guide to prospect assessment. Low enthalpy hydrothermal manifestations are widely distributed in Mexico, some within the active volcanic arc, but also away from it. The latter have been studied marginally (Wolaver et al., 2013; Morales-Arredondo et al., 2018), and the geothermal potential and genesis of high heat flow in areas devoid of active and recent volcanism remains unknown. This is the case for some Miocene-Eocene grabens in central-western Mexico, located far from the active volcanic arc, which have hydrothermal springs with temperatures as high as 74°C.

In this study we propose a preliminary hydrothermal model derived from the analysis of the geochemical properties of water from thermal springs and wells in two of these grabens. Based on the chemical and isotopic characterization of water, we determine the origin of the thermal fluids and relate it to a possible heat source and a heat transference mechanism.

### 2. GEOLOGICAL SETTING

The Juchipila and the Santiago Papasquiaro grabens are located in the southeastern part of the Sierra Madre Occidental (SMO) near its boundary with the Mesa Central physiographic province (Figure 1.A) (Nieto-Samaniego et al., 2005). The SMO is one of the

largest silicic volcanic provinces of the world (Ferrari et al., 2007) and consists of dominantly silicic ignimbrites with less rhyolitic domes and fissural basaltic flows formed from 38 to 20 Ma, which overlie the Late Cretaceous to Eocene Laramide magmatic arc and an older Mesozoic-Paleozoic basement. The volcanic stratigraphy in these grabens includes a thick succession of silicic ignimbrites with thickness up to 1 km. Most of these ignimbrites were vented from fissures associated with the regional extensional fault systems (Ferrari et al., 2007). The last volcanic activity in the the Juchipila and Santiago Papasquiaro grabens dates back to ~11 Ma (Loza-Aguirre et al., 2012; Martínez-Resendiz, 2018). These areas are located far north from the Trans-Mexican Volcanic Belt (TMVB), the currently active volcanic arc, where all the currently active geothermal fields are found (Figure 1A). The principal structures in the southern portion of the SMO are normal faults that bound grabens and half grabens with N-S to NNE-SSW trends (Fig. 1B) (Nieto-Samaniego et al., 1999; Ferrari et al., 2007). The time of extension is diachronous, starting in the late Eocene in Santiago Papasquiaro and in mid-Oligocene times in the southern region (Loza-Aguirre et al., 2012; Ferrari et al., 2018). According to Nieto-Samaniego et al. (1999), the Juchipila graben experienced an elongation of 9% and the major faults have a vertical displacement of 1 km. In the Santiago Papasquiaro graben, the vertical displacement reaches 800 m (Loza-Aguirre et al., 2012).

The stratigraphic columns in the Juchipila and Papasquiaro grabens are very similar and consist of a volcano-sedimentary succession made by Eocene sandstone and andesitic lavas flows, Oligocene silicic ignimbrites and rhyolitic domes and basaltic lava flows of late Oligocene or late Miocene age. The Juchipila graben is filled by early Miocene sandstone and conglomerate and late Miocene to early Pliocene lacustrine sediments with thickness up to 300 m (Martínez-Resendiz, 2019). The Santiago Papasquiaro graben is filled with continental sedimentary rocks of late Oligocene to the Quaternary, which reach up to 300 m of thickness (Loza-Aguirre et al., 2012).

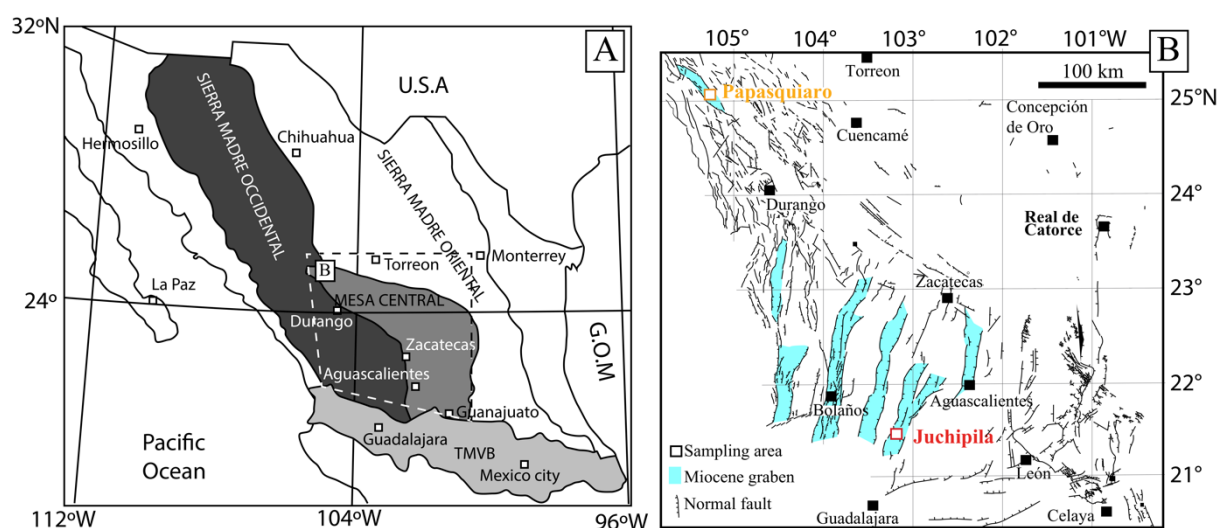


Figure 1: Location of the study areas. Modified from Loza-Aguirre et al., 2008.

### 3. METHODS

Groundwater sampling was conducted in February 2019; the sampling locations were selected according to previous analysis in the study areas. In the Juchipila graben, we collected five water samples from wells (J-06, J-07, J-08, J-11 and J-12) and two from thermal springs (J-09 and J-10). In the Santiago Papasquiaro graben, five water samples from thermal springs (P-13, P-14, P-15, P-18, P-19) and one from river water (P-16) were collected.

Physical-chemical parameters of water (temperature, pH, electrical conductivity, and alkalinity) were measured in situ. Waters for dissolved major ions and O-D isotopes analysis were filtrated with 0.45  $\mu\text{m}$  cellulose acetate membrane filter and stored in high-density polyethylene bottles. In addition, the samples for cation analysis were acidified with  $\text{HNO}_3$ .

Sample waters were collected in 120 ml glass bottles completely filled with water and sealed underwater with rubber septa (except for samples J-04, J-05 and J-07, sampled in lead-glass flasks with two vacuum stopcocks) in order to analyze the chemical and isotope composition of dissolved gases (Capasso and Inguaggiato, 1998).

#### 3.1 Laboratory Analyses

Major ions were analyzed at the Environmental Geochemistry Laboratory at the Centro de Geociencias, UNAM. Anions were determined by high-performance liquid chromatography/ion chromatography (HPLC/IC) with a Dionex ICS-2500®. Cations were determined by inductively coupled plasma optic emission spectrometry (ICP-OES) with a Thermo iCAP 6500 Duo View®.

O-D isotopes were analyzed by isotope ratio laser spectrometry (IRLS) with a liquid water analyzer Los Gatos Research DLT-100 V3® (all samples were filtrated with a 0.2  $\mu\text{m}$  membrane), at the Stable Isotopes laboratory of the National Geochemistry and Mineralogy Laboratory of the Instituto de Geología, UNAM. Noble gas isotopes analysis were performed at the laboratory of the

Istituto Nazionale di Geofisica e Vulcanologia - Palermo. Helium isotopes were analyzed by a Helix SFT-GVI MS, and  $^{20}\text{Ne}$  by a Thermo-Helix MC plus mass spectrometer (Rizzo et al., 2016). The method for the gas extraction and overall analysis is described in detail in Inguaggiato and Rizzo (2004).

The R/Ra values were corrected for atmospheric contamination (Rc/Ra) using the following equation (Hilton, 1996):

$$R_c/R_A = \frac{(R_M/R_A \cdot X) - 1}{X - 1} \quad (1)$$

$$\text{where } X = \frac{(H_e/N_e)_M \beta_{Ne}}{(H_e/N_e)_A \beta_{He}} \quad (2)$$

And where  $\beta_{Ne}$  and  $\beta_{He}$  are the Bunsen solubility coefficients for Ne and He in water.

#### 4. RESULTS

Physical-chemical parameters and major ions chemistry are presented in Table 1. J-06, and SPR-01 represent the cold samples ( $<30^\circ\text{C}$ ) in the studied areas. In the Juchipila graben the maximum temperature reaches  $60.3^\circ\text{C}$ , and in most samples pH is neutral, and the EC is in the 353-1302  $\mu\text{S}/\text{cm}$  range. In the Santiago Papasquiario graben, the thermal springs samples have maximum temperatures of  $74.3^\circ\text{C}$ , most of the samples have neutral pH, and EC values of 287-1195  $\mu\text{S}/\text{cm}$ .

**Table 1: Physicochemical parameters, major ions chemistry and O-D-He isotopes in the Juchipila, and Santiago Papasquiario grabens**

| Sample                       | T<br>(°C) | pH  | EC <sup>a</sup> | Major Ions <sup>b</sup> |     |      |      |      |                 | Trace elements <sup>b</sup> |       |       |      |       |
|------------------------------|-----------|-----|-----------------|-------------------------|-----|------|------|------|-----------------|-----------------------------|-------|-------|------|-------|
|                              |           |     |                 | Na                      | K   | Ca   | Mg   | Cl   | SO <sub>4</sub> | alk.                        | Li    | As    | F    | B     |
| Juchipila graben             |           |     |                 |                         |     |      |      |      |                 |                             |       |       |      |       |
| J-01                         | 35        | 6.9 | 398             | 62.5                    | 3.6 | 25.8 | 0.30 | 7.1  | 10.3            | 184                         | 0.071 | <LoQ  | 1.0  | 0.074 |
| J-02                         | 37.7      | 7.8 | 390             | 69.8                    | 2.7 | 17.2 | 0.20 | 4.8  | 10.6            | 171                         | 0.124 | <LoQ  | 2.7  | 0.172 |
| J-03                         | 41.2      | 8.3 | 612             | 124.6                   | 1.5 | 5.3  | 0.05 | 15.5 | 48.5            | 196                         | 0.263 | 0.045 | 8.4  | 0.792 |
| J-04                         | 45.1      | 8.2 | 647             | 128.1                   | 1.5 | 5.4  | 0.07 | 19.6 | 68.7            | 180                         | 0.246 | 0.053 | 11.3 | 0.969 |
| J-05                         | 60.3      | 8.6 | 1302            | 207.0                   | 5.2 | 23.9 | 0.23 | 64.4 | 294.4           | 136                         | 0.498 | 0.163 | 9.1  | 2.211 |
| J-06                         | 25.3      | 7.1 | 424             | 25.1                    | 6.1 | 59.5 | 5.90 | 2.6  | 6.6             | 196                         | 0.023 | <LoQ  | 0.4  | 0.032 |
| J-07                         | 29.7      | 7.6 | 353             | 38.8                    | 6.7 | 33.9 | 1.42 | 5.4  | 7.3             | 166                         | 0.076 | <LoQ  | 2.1  | 0.048 |
| Santiago Papasquiario graben |           |     |                 |                         |     |      |      |      |                 |                             |       |       |      |       |
| SP-01                        | 68.8      | 7.2 | 629             | 104.4                   | 4.4 | 11.7 | 0.02 | 13.7 | 89.6            | 120                         | 0.640 | 0.112 | 7.8  | 0.605 |
| SP-02                        | 69.1      | 7.0 | 603             | 103.5                   | 4.2 | 12.2 | 0.04 | 19.7 | 80.1            | 180                         | 0.628 | 0.143 | 7.0  | 0.617 |
| SP-03                        | 63.9      | 7.3 | 543             | 97.3                    | 3.9 | 12.3 | 0.04 | 11.4 | 79.1            | 157                         | 0.547 | 0.130 | 7.2  | 0.527 |
| SPR-01                       | 20.8      | 8.8 | 287             | 36.4                    | 3.9 | 20.2 | 1.74 | 6.0  | 27.4            | 110                         | 0.122 | 0.042 | 1.8  | 0.148 |
| SP-04                        | 74.3      | 6.5 | 1195            | 213.1                   | 9.6 | 13.3 | 0.58 | 14.4 | 129.6           | 375                         | 0.563 | 0.104 | 9.7  | 0.958 |
| SP-05                        | 42.3      | 9.4 | 334             | 66.5                    | 0.4 | 2.9  | 0.06 | 4.4  | 33.6            | 113                         | 0.117 | 0.091 | 3.6  | 0.181 |

a. EC: electrical conductivity in  $\mu\text{S}/\text{cm}$ .

b. Major ions and trace elements concentration in mg/l

<LoQ = below limit of quantification.

#### 4.1 Water Chemistry

The Piper diagram (Figure 2) shows the anion and cation proportions as a percentage from their concentration in meq/L and distinguishes different groups of water.

The thermal waters (>30°C) in the Juchipila graben have compositions evolving from Na-HCO<sub>3</sub> to Na-SO<sub>4</sub>. High values of EC and enrichment of SO<sub>4</sub> occur mainly in the central and southern portion of the graben. The SO<sub>4</sub> enrichment is related to a greater thickness of the lacustrine sediments and agriculture activities. In the Santiago Papasquiaro graben, the composition is mainly Na-HCO<sub>3</sub>, and the samples have lower concentrations of Cl. The thermal groundwater samples in both grabens have anomalous concentrations of F, B, Li, and As, which are related to rock dissolution and alteration processes. This enrichment has been reported in other areas in Mexico. They are usually interpreted as the result of water/rock interaction processes entailing ignimbrites and volcanic glass in a deep fractured regional aquifer (Shaw and Sturchio, 1992; Alarcón-Herrera et al., 2013; Morales-Arredondo et al., 2016).

The cold sample in the Juchipila graben has a Ca-HCO<sub>3</sub> composition, while in the Santiago Papasquiaro graben it is slightly enriched in SO<sub>4</sub>. All cold samples have low EC values and are interpreted as the recent recharge or superficial water.

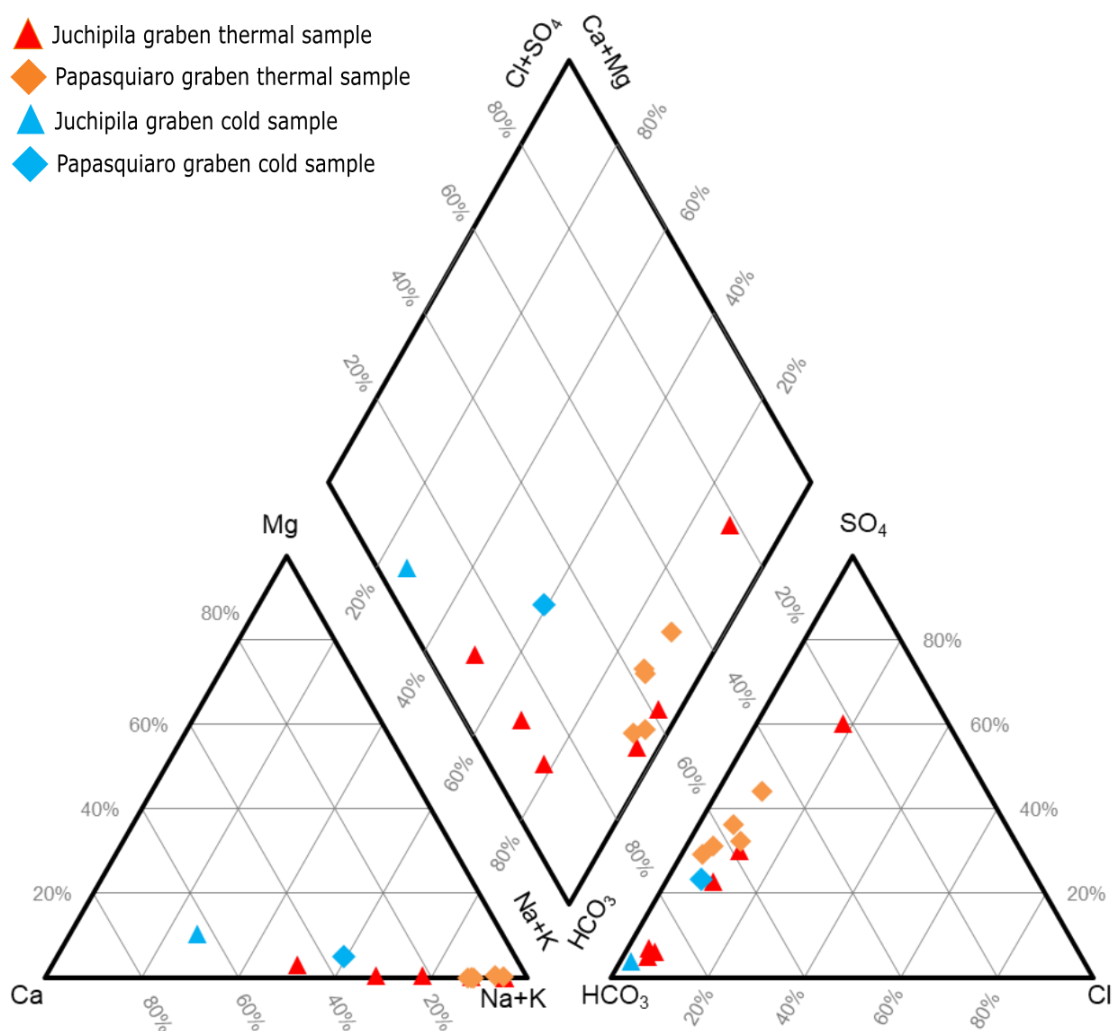


Figure 2: Piper diagram of the water samples of the Juchipila, and Papasquiaro grabens.

#### 4.2 O-D Isotopes

The  $\delta^2\text{H}$  and  $\delta^{18}\text{O}$  of the samples are plotted in Figure 3, along with the global meteoric water line (GMWL) and a local evaporation line constructed with thermal and cold samples of the Juchipila and Papasquiaro grabens (Billarent-Cedillo, 2019). The dotted curve shows a mixture with andesitic water in a typical volcanic geothermal field, like Los Azufres, located in the central Trans-Mexican Volcanic Belt.

In the Santiago Papasquiario graben, the thermal samples fall along the GMWL, while the river sample is highly evaporated. In the Juchipila graben, the thermal and cold samples fall close to the GMWL. All are distributed along a common local evaporation line. The hottest samples show less evaporation evidences. In the Figure 3, the  $\delta^2\text{H}$  and  $\delta^{18}\text{O}$  isotopic results clearly suggest that both geothermal systems are dominated by meteoric waters, excluding any participation or a mixture with volcanic waters.

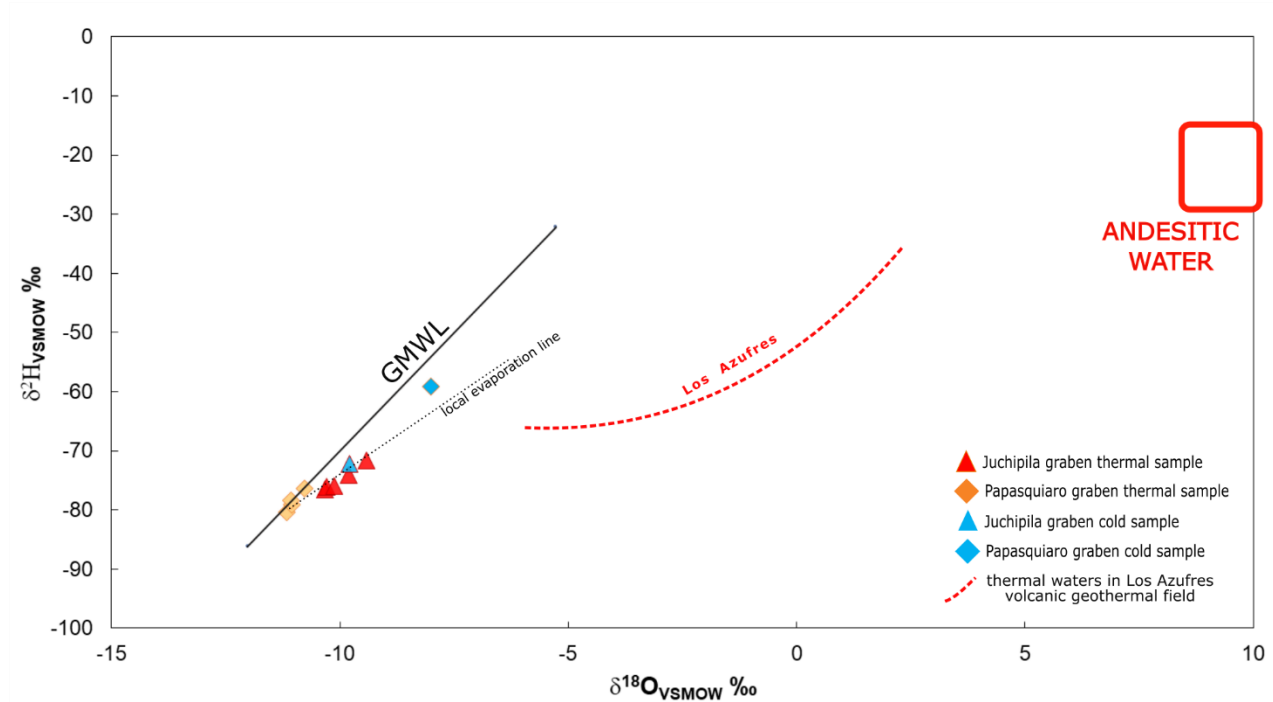


Figure 3:  $\delta^{18}\text{O}$  vs.  $\delta^2\text{H}$  diagram of the water samples of the Juchipila and Santiago Papasquiario grabens.

#### 4.3 He Isotopes

The  $^3\text{He}/^4\text{He}$  ratios measured in the sample (R) were normalized to the  $^3\text{He}/^4\text{He}$  ratio in the air ( $R_a = 1.384 \cdot 10^{-6}$ , Clarke et al., 1976).

The dissolved gas samples of thermal waters in the Juchipila graben have  $^4\text{He}$  concentrations up to  $6.09 \cdot 10^{-3}$  cc/l and  $R_c/R_a$  values ranging from 0.24 to 1.36. The thermal samples of the Papasquiario graben present high  $^4\text{He}$  concentrations up to  $7.16 \cdot 10^{-3}$  cc/l and  $R_c/R_a$  values from 0.18 to 0.72.

The  $R/R_a$  ratio versus the  $^4\text{He}/^{20}\text{Ne}$  ratio for each sample is plotted in Figure 4. Derived from the fact that the  $R/R_a$  composition is different for the unique terrestrial reservoirs (atmosphere, mantle and crust), and as  $^{20}\text{Ne}$  concentration comes only from the atmosphere, a proportion of He from each end-member can be calculated for the dissolved gas samples (Sano and Wakita, 1985). The end-members of  $R/R_a$  used for the calculations are: Air saturated water (ASW) = 0.983  $R_a$ , crust = 0.02  $R_a$  and mantle = 7  $R_a$  (Benson and Krause, 1980; Sano and Marty, 1995; Kennedy et al., 2007; Inguaggiato et al., 2016). The end-members of the  $^4\text{He}/^{20}\text{Ne}$  ratios used for the calculations are for ASW = 0.285, crust and mantle = 1000 (Sano and Wakita, 1985).

In the Juchipila graben, all analyzed samples have high proportion of ASW end-member (28-86%) and crustal end-member (12-58%), however, the mantle He contribution is significative, up to 14%. In the Santiago Papasquiario graben the mantle He contribution is lower, up to 9%, the ASW proportion is low (1-22%), and the crustal helium contribution is higher (76-96%) with respect to the Juchipila graben.

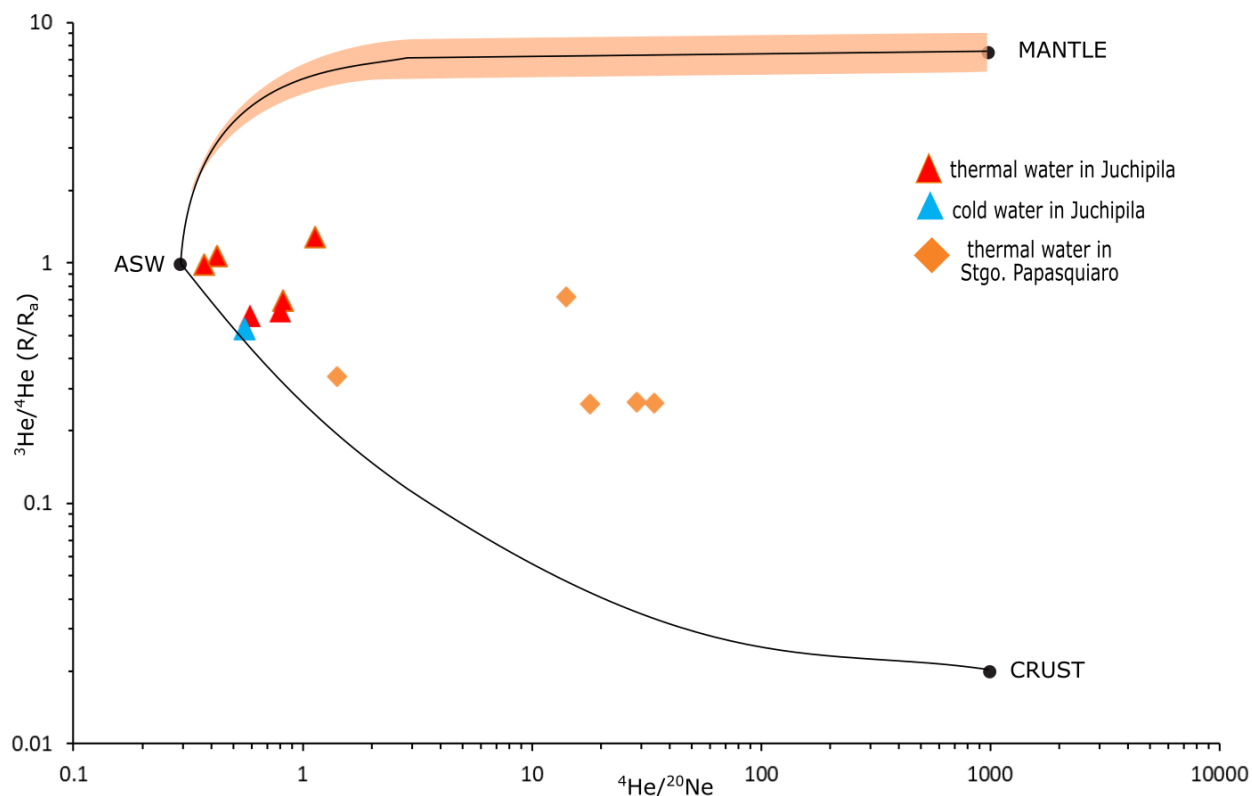


**Figure 4:**  $^4\text{He}/^{20}\text{Ne}$  vs.  $R/R_a$  diagram of the dissolved gas samples of the Juchipila and Papasquiario grabens. ASW: Air saturate water.

## 5. DISCUSSION

Based on the physical-chemical water characteristics in Juchipila and Santiago Papasquiario graben, two water families could be identified: one with a low temperature and  $\text{Ca-HCO}_3$  composition and another with high temperature and  $\text{Na-HCO}_3\text{-SO}_4$  composition. O-D isotope ratios clearly indicate a common meteoric source for both families but subject to different hydrological processes. Physical-chemical features of water samples and O-D isotopes suggest that the hot water recharge is fast and interacts with volcanic rocks. We propose preliminarily that rainwater moves through the fault network into the fractured basement at 3–4 km of depth, dissolving mantle and crustal helium as it gets heated by the geothermal gradient. This depth is proposed in accordance with the magneto-telluric soundings in the Juchipila graben (Ávila-Vargas, 2019), and the geothermometric reservoir temperatures of 85°C in the Juchipila graben and 105°C in the Santiago Papasquiario graben (Billarent-Cedillo, 2019). Cold groundwater and springs show a higher evaporation grade than the hot spring waters, suggesting more extended run-off and longer residence time within shallow conglomerate and carbonate host rock. During the return to the surface along high-permeability fault-associated pathways the hot groundwater endmembers get mixed with the shallower and cold aquifer within the valley filling sediments.

The samples in Juchipila graben and Santiago Papasquiario graben have  $^4\text{He}/^{20}\text{Ne}$  ratios higher than the ASW end-member, due to the contribution of fluids derived from crust and mantle. In particular, the samples in the Santiago Papasquiario graben have  $^4\text{He}/^{20}\text{Ne}$  ratios higher than Juchipila graben, and crustal He proportion from 80 to 96% with atmospheric contribution less than 2% (except in sample SP-05). The high  $^4\text{He}$  concentration is generally related to the  $\alpha$  decay of U and Th (Graham, 2002), in good agreement with the several U anomalies reported in the Santiago Papasquiario graben and surroundings (Villarreal et al., 2011). Mantle degassing in the Juchipila graben is not surprising because of the importance of the basement involved faulting during the graben formation and its close position to the Mesa Central boundary, the crustal Tepehuanes fault corridor, and the occurrence of subcrustal asthenosphere (Nieto Samaniego et al., 2005).

## 6. CONCLUSIONS

In this study, two low enthalpy hydrothermal occurrences in central-western Mexico were characterized for the first time by means of their chemical composition, O-D and He isotopes. The thermal waters in the Juchipila graben have a  $\text{Na-HCO}_3$  and  $\text{Na-SO}_4$  composition, and in the Santiago Papasquiario graben, they have a  $\text{Na-HCO}_3$  composition. In the study areas, the O-D isotopes in springs and groundwater illustrate the importance of the meteoric recharge. The He isotopes dissolved in waters coupled with  $^4\text{He}/^{20}\text{Ne}$  ratios show that mantle- and crust-derived helium is dissolved in thermal waters collected in Papasquiario and Juchipila graben. In the Juchipila graben a higher mantle helium contribution up to 14% was identified, while in Papasquiario graben lower mantle He proportion up to 9% was recognized.

The findings of mantle derived helium in Papasquiario and Juchipila area allow proposing that deep faults could facilitate the upflow of mantle helium. Moreover, in Papasquiario graben the high contribution of radiogenic helium, up to 96%, can be justified

by the anomalous concentrations of U and Th in the local rocks. Further studies and data processing can allow to propose a geothermal model of the investigated areas .

Research funded by grant PAPIIT IV100117.

## REFERENCES

- Alarcón-Herrera, M. T., Bundschuh, J., Nath, B., Nicolli, H.B., Gutierrez M., Reyes-Gomez V.M., Nuñez, D., Martín-Dominguez, I.R., Sracek, O.: Co-occurrence of arsenic and fluoride in groundwater of semi-arid regions in Latin America: Genesis, mobility and remediation. *Journal of Hazardous Materials*, 262, (2013) 960-969. <https://doi.org/10.1016/j.jhazmat.2012.08.005>
- Avila-Vargas O.: Modelo del Graben de Juchipila a partir de datos magnetotélúricos. Tesis de Maestría. Universidad Nacional Autónoma de México. (master's thesis), Universidad Nacional Autónoma de México (2019)
- Benson, B. B., & Krause, D.: Isotopic fractionation of helium during solution: A probe for the liquid state. *Journal of Solution Chemistry*, 9(12), (1980), 895–909. <https://doi.org/10.1007/BF00646402>
- Billarent-Cedillo, A.: Origen y flujo de aguas termales en sistemas geotérmicos de baja entalpía en los grábenes de Juchipila y Santiago Papasquiaro: caracterización hidroquímica e isotópica (O-H; He). (master's thesis), Universidad Nacional Autónoma de México (2019)
- Capasso, G., & Inguaggiato, S., 1998 : A simple method for the determination of dissolved gases in natural waters. An application to thermal waters from Vulcano Island. *Applied Geochemistry*, 13(5), (1998), 631–642. [https://doi.org/10.1016/S0883-2927\(97\)00109-1](https://doi.org/10.1016/S0883-2927(97)00109-1)
- Clarke, W. B., Jenkins, W. J., & Top, Z.: Determination of tritium by mass spectrometric measurement of  $3\text{He}$ . *The International Journal of Applied Radiation and Isotopes*, 27(9), (1976), 515–522. [https://doi.org/10.1016/0020-708X\(76\)90082-X](https://doi.org/10.1016/0020-708X(76)90082-X)
- Ferrari, L., Valencia-Moreno, M., & Bryan, S. : Magmatism and tectonics of the Sierra Madre Occidental and its relation with the evolution of the western margin of North America. En *Special Paper 422: Geology of México: Celebrating the Centenary of the Geological Society of México* Vol. 422, (2007). pp. 1-39. [https://doi.org/10.1130/2007.2422\(01\)](https://doi.org/10.1130/2007.2422(01))
- Ferrari, L., Orozco-Esquivel, T., Bryan, S. E., López-Martínez, M., & Silva-Fragoso, A.: Cenozoic magmatism and extension in western Mexico\_ Linking the Sierra Madre Occidental silicic large igneous province and the Comondú Group with the Gulf of California rift. *Earth Science Reviews*, 183, (2018): 115–152. <http://doi.org/10.1016/j.earscirev.2017.04.006>
- Flores-Armenta, M., Ramírez-Montes, M., & Morales-Alcalá, L.: Geothermal activity and development in Mexico – Keeping the production going (2012).
- Graham: Donald P. Porcelli, Chris J. Ballentine, and Rainer Wieler , editors - Noble gases in geochemistry and cosmochemistry Reviews in mineralogy and geochemistry, (2002) Mineralogical Society of America
- Gutierrez-Negrin, L. C. A., Maya-Gonzalez, R., & Quijano-Leon, J. L.: *Present Situation and Perspectives of Geothermal in Mexico*. 10 (2015).
- Hilton, D. R.: The helium and carbon isotope systematics of a continental geothermal system: results from monitoring studies at Long Valley caldera (California, USA)." *Chemical Geology* 127.4 (1996): 269-295.
- Iglesias E. R., Torres R. J., Martínez-Estrella I. J., Reyes-Picasso N.: Summary of the 2010 Assessment of Medium-to Low-Temperature Mexican Geothermal Resources. *Geothermal Resources Council Transactions* 34, (2010) 1155-1159.
- Inguaggiato, S., Rizzo, A.: Dissolved helium isotope ratios in ground-waters: a new technique based on gas–water re-equilibration and its application to Stromboli volcanic system. *Appl. Geochem.* 19 (2004): 665–673.
- Inguaggiato, C., Censi, P., D'Alessandro, W., & Zuddas, P.: Geochemical characterisation of gases along the dead sea rift: Evidences of mantle- $\text{CO}_2$  degassing. *Journal of Volcanology and Geothermal Research*, 320, (2016): 50–57. <https://doi.org/10.1016/j.jvolgeores.2016.04.008>
- Kennedy, B. M., & van Soest, M. C. Flow of Mantle Fluids Through the Ductile Lower Crust: Helium Isotope Trends. *Science*, 318(5855), (2007), 1433-1436. <https://doi.org/10.1126/science.1147537>
- Loza Aguirre, I.: Cenozoic volcanism and extension in northwestern Mesa Central, Durango, México. *Boletín de La Sociedad Geológica Mexicana*, 64(2), (2012), 243-263. <https://doi.org/10.18268/BSGM2012v64n2a9>
- Martínez-Resendiz, E.V.: Estudio Geológico de la parte sur del graben de Juchipila. Reunión Anual UGM 2018 SE-01-10 (2018), 0484.



- Morales-Arredondo, I., Rodríguez, R., Armienta, M. A., & Villanueva-Estrada, R. E.: The origin of groundwater arsenic and fluorine in a volcanic sedimentary basin in central Mexico: a hydrochemistry hypothesis. *Hydrogeology Journal*, 24(4), (2016), 1029-1044. <https://doi.org/10.1007/s10040-015-1357-8>
- Morales-Arredondo, J. I., Esteller-Alberich, M. V., Armienta Hernández, M. A., & Martínez-Florentino, T. A. K.: Characterizing the hydrogeochemistry of two low-temperature thermal systems in Central Mexico. *Journal of Geochemical Exploration*, 185, (2018), 93-104. <https://doi.org/10.1016/j.gexplo.2017.11.006>
- Nieto-Samaniego, Á. F., Ferrari, L., Alaniz-Alvarez, S. A., Labarthe-Hernández, G., & Rosas-Elguera, J.: Variation of Cenozoic extension and volcanism across the southern Sierra Madre Occidental volcanic province, Mexico. *Geological Society of America Bulletin*, 111(3), (1999), 347-363.
- Nieto-Samaniego, Ángel F., Alaniz-Alvarez, S. A., Camprubí A.: La Mesa Central de México: estratigrafía, estructura y evolución tectónica cenozoica. *Boletín de la Sociedad Geológica Mexicana LVII*, núm. 3, (2005), p. 285-318
- Rizzo, A. L., Caracausi, A., Chavagnac, V., Nomikou, P., Polymenakou, P. N., Mandalakis, M.: Kolumbo submarine volcano (Greece): An active window into the Aegean subduction system. *Scientific Reports*, 6(1), (2016), 1–9. <https://doi.org/10.1038/srep28013>
- Sano, Y., & Marty, B.: Origin of carbon in fumarolic gas from island arcs. *Chemical Geology (Isotope Geoscience Section)*, 119, (1995), 265–274. [https://doi.org/10.1016/0009-2541\(94\)00097-R](https://doi.org/10.1016/0009-2541(94)00097-R)
- Sano, Y., & Wakita, H.: Geographical distribution of  $^3\text{He}/^4\text{He}$  ratios in Japan: Implications for arc tectonics and incipient magmatism. *Journal of Geophysical Research*, 90(B10), (1985), 8729–8741. <https://doi.org/10.1029/JB090iB10p08729>
- Shaw, D. M., & Sturchio, N. C.: Boron-lithium relationships in rhyolites and associated thermal waters of young silicic calderas, with comments on incompatible element behaviour. (1992), [https://doi.org/10.1016/0016-7037\(92\)90165-F](https://doi.org/10.1016/0016-7037(92)90165-F)
- Villarreal, J., Levresse, G., Corrona, R., Tritla, J., Sanchez, N.: Principales anomalías de uranio en México. In book: XXIX Convención Internacional de Minería AIMMG, AC., Publisher: Asociación de Ingenieros de Minas, Metalurgistas y Geólogos de México, Editors: Rodolfo Corona-Esquivel, J.A. Gómez-Caballero, (2011), pp.255-259
- Wolaver, B. D., Crossey, L. J., Karlstrom, K. E., Banner, J. L., Cardenas, M. B., Ojeda, C. G., & Sharp Jr, J. M.: Identifying origins of and pathways for spring waters in a semiarid basin using He, Sr, and C isotopes: Cuatrociénegas Basin, Mexico. *Geosphere*, 9(1), (2013), 113-125.